national accelerator laboratory

NAL-Pub-74/14-THY
January 1974

Possible Effects of Weakly Coupled Neutral Currents in pp $\to \ell^+\ell^- + X$

R. W. BROWN,* K. O. MIKAELIAN*
Case Western Reserve University, Cleveland, Ohio 44106

and

MARY K. GAILLARD†
National Accelerator Laboratory, Batavia, Illinois 60510

ABSTRACT

We discuss the possibility of observing weak neutral currents in the inclusive production of ordinary lepton pairs in high energy proton-proton collisions. Our signatures of interest are the charge asymmetry $\langle E_{\ell^+} - E_{\ell^-} \rangle$ and the polarization of the leptons. The weak interaction is considered to be mediated by a neutral vector boson and the calculations are done in the parton model. This model is also used to estimate the asymmetry background due to two-photon exchange. To obtain numerical results we use weak couplings suggested by the Weinberg theory.

*Supported in part by the National Science Foundation, Grant No. GP-33119.

†On leave of absence from L. P. T. P. E., Orsay (Laboratoire associé an CNRS).

I. INTRODUCTION

With the proliferation of gauge theories which unify weak and electromagnetic interactions has come a renewal of interest in weakly coupled neutral currents and bosons.[1] If tentative evidence[2] for neutral currents in neutrino reactions is not confirmed by subsequent experiments, it will become even more imperative to search for neutral currents which are coupled neither to neutrinos nor to a $|\Delta S| = 1$ hadronic system. Heretofore, there has been no firm evidence[3] for such interactions, let alone for the existence of a weak neutral vector boson. The possibility[3]--and perhaps necessity[4]--of a large mass for this boson blurs our view of production experiments and so attention is usually focused on the virtual effects.[5]

We discuss here some of these effects as they pertain to the inclusive lepton pair production reaction

$$p + p \rightarrow \ell^+ + \ell^- + X \qquad \text{(i)}$$

Besides the colliding proton beams at ISR, we have in mind the higher energy machines proposed for the future.[6] The question of interest is whether or not neutral currents can be observed via Reaction (i).

Reaction (i) is well-known for its relevance to the parton model.[7] While the results of parton models for other processes like deep inelastic lepton-nucleon scattering or electron-positron annihilation into hadrons are corroborated by studies of current products on the light cone, the same is not true for Reaction (i). Moreover, the scaling predicted by the parton model for this reaction has not yet been verified since the experiments at ISR and at Brookhaven[8] do not overlap in the scaling variable r (defined in the next section). But the model is yet innocent of misleading us and calculations are simple enough (the extension of gauge theories to include hadrons is quite straightforward here) so we will use it.

Two weak effects are considered. In Sec. II, we derive an expression for the charge asymmetry between ℓ^+ and ℓ^- if one has a vector boson coupled weakly to the leptons and quarks. Since two-photon exchange also induces such an asymmetry, an expression is found for that contribution as well. Polarization is a clear-cut indication of parity-violating weak effects and so the lepton helicity is examined in Sec. III. More specific assumptions about the parton and gauge models are needed for numerical estimates and we present these in Sec. IV. A few concluding remarks make up Sec. V.

II. CHARGE ASYMMETRY

A parton analysis[7] of Reaction (i), $pp \to \ell^+ \ell^- X$, tells us that the dominant contribution at large lepton-pair invariant mass $\sqrt{Q^2}$ corresponds to parton-antiparton annihilation into a highly virtual photon which in turn decays into $\ell^+ \ell^-$ (Fig. 1a). Requiring partons to remain close to their mass shell, bremsstrahlung diagrams (Fig. 1b) vanish relative to the annihilation diagrams and we obtain the well-known scaling behavior:

$$\frac{d\sigma}{dQ^2} = \frac{1}{(Q^2)^2} f\,(Q^2/s) \tag{2.1}$$

where s $\equiv$ square of the c.m. energy in Reaction (i).

In the one-photon approximation, charge asymmetries like $<E_{\ell^+} - E_{\ell^-}>$ vanish. Interference terms arising from additional parity-violating or higher-order electromagnetic amplitudes can, on the other hand, produce certain charge asymmetries. It is precisely these effects which we examine in this section where the additional amplitudes are due to weak neutral boson and two-photon exchanges. A crude use of the aforementioned parton analysis enables us to get a handle on the strong interactions.

If $P_i(x)$ is the probability of finding the i^{th} type of quark in the proton with fraction x of its longitudinal momentum, the inclusive cross section for pair production is

$$d\sigma = \sum_i \int dx\, dx'\; P_i(x)\, P_{\bar{i}}\,(x')\, d\sigma_i \tag{2.2}$$

where $d\sigma_i$ is the differential cross section for $q_i q_{\bar{i}} \rightarrow \ell^+ \ell^-$. We use the following interaction Lagrangian to calculate $d\sigma_i$:

$$\mathscr{L}_{int} = -e\,\bar{\ell}\,\gamma_\mu\,\ell\,A^\mu - m_z\left(\frac{G}{\sqrt{2}}\right)^{\frac{1}{2}}\;\bar{\ell}\;\gamma_\mu(a+b\gamma_5)\,\ell\;Z^\mu$$

$$+ \sum_i [\,e\,Q_i\,\bar{q}_i\,\gamma_\mu q_i A^\mu - m_z\left(\frac{G}{\sqrt{2}}\right)^{\frac{1}{2}}\;\bar{q}_i\;\gamma_\mu(a_i+b_i\gamma_5)q_i\,Z^\mu\,] \tag{2.3}$$

in terms of $G \cong 10^{-5} m^{-2}_{proton}$, m_Z = neutral vector boson mass, and Q_i = electric charge on the i^{th} type of quark. The relative vector and axial-vector weights determined by the a's and b's vary according to the weak interaction model employed.

To lowest order in $\alpha \equiv e^2/4\pi$ and G, (2.3) leads to

$$\frac{d\sigma_i}{d\cos\theta} = \frac{\pi\alpha^2}{2Q^2}\Big\{Q_i^2(1+\cos^2\theta) + 2Q_iR(Q^2)[aa_i(1+\cos^2\theta) + 2bb_i\cos\theta] + R^2(Q^2)[(a^2+b^2)(a_i^2+b_i^2)(1+\cos^2\theta) + 8ab\,a_ib_i\cos\theta]\Big\} \tag{2.4}$$

where θ is the angle between the parton q_i and the lepton ℓ^- in the di-lepton c.m. and

$$R(Q^2) \equiv \frac{G\,Q^2/\sqrt{2}}{4\pi\alpha\left(1 - \frac{Q^2}{m_Z^2}\right)} . \tag{2.5}$$

Save for m_Z, all mass terms have been neglected in Eq. (2.4) in view of our interest in very large S and Q^2.

Let us denote the $\ell^\pm$ four-momenta by $p_\pm$. Then $Q = p_+ + p_-$ and define $q \equiv p_- - p_+$. If $Q_\parallel$ and $q_\parallel$ stand for components parallel to the beam in the overall (pp) c.m. system, then $Q_+ \equiv Q_0 + Q_\parallel$ and $q_+ \equiv q_0 + q_\parallel$. With the further definitions $r \equiv \frac{Q^2}{s}$ and $y \equiv \frac{1}{2}(1 + \frac{q_+}{Q_+})$, we have

$$xx' = r,$$

$$\cos\theta = 2y - 1,$$

$$q_0 = \frac{1}{2}\sqrt{s}\ x\,(2y-1)(1-r/x^2),$$
$$q_{\parallel} = \frac{1}{2}\sqrt{s}\ x\,(2y-1)(1+r/x^2),$$
$$Q_{\parallel} = \frac{1}{2}\sqrt{s}\ x\,(1-r/x^2)\,, \qquad (2.6)$$

in the approximation which neglects masses (muon, quark, and proton). The portion of the ranges $0 \le r \le 1$, $0 \le y \le 1$, and $r \le x \le 1$ corresponding to $q_0 > 0$, $q_{\parallel}/Q_{\parallel} > 0$ is $y > \frac{1}{2}$, $x > \sqrt{r}$ or $y < \frac{1}{2}$, $x < \sqrt{r}$.

We can now write the charge asymmetry of interest for fixed Q^2:

$$A = \frac{\frac{d\sigma}{dr}(q_0 > 0) - \frac{d\sigma}{dr}(q_0 < 0)}{\frac{d\sigma}{dr}} = \frac{\frac{d\sigma}{dr}(q_{\parallel}/Q_{\parallel} > 0) - \frac{d\sigma}{dr}(q_{\parallel}/Q_{\parallel} < 0)}{\frac{d\sigma}{dr}} \qquad (2.7)$$

The relationship between A and $<E_{\ell_+} - E_{\ell_-}> = -<q_0>$ should be clear. Looking back at Eq. (2.4), the cross section ingredients in Eq. (2.7) are

$$\frac{d\sigma}{dr} = \frac{8\pi\alpha^2}{Q^2} \sum_i{}' \left[Q_i^2 + 2R(Q^2)a\,a_i Q_i + R^2(Q^2)(a^2+b^2)(a_i^2+b_i^2)\right]$$
$$\times \int_{\sqrt{r}}^{1} \frac{dx}{x}\left[I_i(r,x) + I_{\bar{i}}(r,x)\right] \int_{y_0}^{1-y_0} y^2\,dy \qquad (2.8)$$

and

$$\frac{d\sigma}{dr}(q_0 > 0) - \frac{d\sigma}{dr}(q_0 < 0) = \frac{d\sigma}{dr}(q_{\parallel}/Q_{\parallel} > 0) - \frac{d\sigma}{dr}(q_{\parallel}/Q_{\parallel} < 0)$$

$$= -\frac{16\pi\alpha^2}{Q^2} R(Q^2) \sum_i{}' \left[b b_i Q_i + 2R(Q^2) a b a_i b_i\right] \int_{\sqrt{r}}^{1} \frac{dx}{x}\left[I_i(r,x) - I_{\bar{i}}(r,x)\right]$$

$$\times \int_{1/2}^{1-y_0} (1 - 2y)\, dy \,. \tag{2.9}$$

Only terms odd under $\theta \to \pi - \theta$ have contributed to (2.9). Use has been made of the charge conjugation properties of currents which imply $b_{\bar{i}} Q_{\bar{i}} = -b_i Q_i$ and $a_{\bar{i}} b_{\bar{i}} = -a_i b_i$, so the sums are only over quark states. We have introduced

$$I_i(r, x) \equiv P_i(x)\, P_{\bar{i}}(r/x) \tag{2.10}$$

and $y_0 = y_0(x) = y_0(r/x)$, a possible experimental cutoff on the lepton angle [or on the transverse momentum related to y through $p_\perp^2 = rsy(1-y)$]. If no cutoff is present, $y_0 = 0$.

A numerical estimate of Eqs. (2.8) and (2.9)--and hence A^{Weak}--using a specific model for the weak neutral currents will be given in Sec. IV. The remaining formula development to be done here involves the higher order electromagnetic contributions to A.

The interference between two-photon exchange and one-photon exchange and between the amplitudes for hadron bremsstrahlung and muon bremsstrahlung give rise to a charge asymmetry A^{EM} of order α. No general method (phenomenological or otherwise) exists which can be used in the evaluation of the two-photon hadronic form factors; however, we have reason to believe that better than an order-of-magnitude estimate is achieved within a quark model. (The relevant quark model amplitudes for two-photon exchange, hadron bremsstrahling, and muon bremsstrahlung are illustrated in Fig. 2.) That is, the infrared contribution dominates the charge asymmetry in, for example, $e^+e^- \to \mu^+\mu^-$,[9,10] corresponding to the virtual integration regions where one of the two photon exchanged is soft (the other necessarily very hard) and to the soft-bremsstrahlung phase space region. This contribution is the residue of the infrared divergence cancellation. Since these long-wavelength photons interact only with the charge of the given particle, it will be consistent to treat the quarks as pointlike here as well. In short, all of our photons are either very hard or very soft, both interacting with point particles.

What about graphs where the two photons (real or virtual) are not connected to the same quark? These are not infrared divergent and are to be neglected in a first estimate. It is the quark which has been violently decelerated (annihilated) which is assumed likely to radiate.[11] Other contributions will be mentioned in Sec. V.

In consequence we have an easy time of it. Some earlier work[9,10] can be carried over with minor change (quarks and leptons have opposite charge assignments) and we have

$$\frac{d\sigma_i}{d\cos\theta} = -\frac{2\alpha^3}{Q^2} Q_i^3\, F(y) + \text{terms symmetric in } \cos\theta + 0(\alpha^4)$$

where

$$F(y) = (1 + \cos^2\theta)\ [\,2\,\ell n \tan\frac{\theta}{2}\ \ell n\ \frac{\Delta E}{E} + \ell n^2 \sin\frac{\theta}{2} - \ell n^2 \cos\frac{\theta}{2}$$

$$+ \frac{1}{2}\,\mathrm{Li}_2(\cos^2\frac{\theta}{2}) - \frac{1}{2}\,\mathrm{Li}_2(\sin^2\frac{\theta}{2})\,] - \cos\,\theta\,(\ell n^2 \sin\frac{\theta}{2} + \ell n^2 \cos\frac{\theta}{2})$$

$$- \sin^2\frac{\theta}{2}\,\ell n \cos\frac{\theta}{2} + \cos^2\frac{\theta}{2}\,\ell n \sin\frac{\theta}{2}\,. \qquad (2.11)$$

The energy resolution of the detectors (both muons are detected) has been taken to be the same, $\frac{\Delta E}{E} = 10\%$ for our numerical work. The soft-photon approximation implicit in (2.11) is expected to be rather accurate.[12] Going on, we obtain

$$\frac{d\sigma}{dr}(q_0 > 0) - \frac{d\sigma}{dr}(q_0 < 0) = -\frac{16\alpha^3}{Q^2}\sum_i{}' Q_i^3 \int_{\sqrt{r}}^{1} \frac{dx}{x}\,[\,I_i(r,x) - I_{\bar{i}}(r,x)\,] \int_{1/2}^{1-y_0} F(y)\,dy. \qquad (2.12)$$

Numerical results for A^{EM} using a specific parton model will be given in Sec. IV.

III. LEPTON POLARIZATION

For comparison with an experiment which measures the helicity h of one of the leptons, it is necessary to undo the lepton polarization sum implicit in Eq. (2.4). Continuing to neglect the lepton and quark masses, we find

$$\frac{d\sigma_i^h}{d\cos\theta} = \frac{1}{2}\,\frac{d\sigma_i}{d\cos\theta} + \frac{\pi\alpha^2 R(Q^2)}{2Q^2}\,h\,\Big\{ Q_i\,[\,ba_i\,(1+\cos^2\theta) + 2ab_i\cos\theta\,]$$

$$+ R(Q^2)\,[\,ab(a_i^2 + b_i^2)(1+\cos^2\theta) + 2a_i b_i(a^2+b^2)\cos\theta\,]\Big\} \qquad (3.1)$$

where $\frac{d\sigma_i}{d\cos\theta} = \frac{d\sigma^{h=1}}{d\cos\theta} + \frac{d\sigma^{h=-1}}{d\cos\theta}$ is given by (2.4).

Hence, in terms of the inclusive cross section, the average helicity is

$$\langle h\rangle \equiv \frac{\frac{d\sigma}{dr}^{h=1} - \frac{d\sigma}{dr}^{h=-1}}{\frac{d\sigma}{dr}} \tag{3.2}$$

and, according to (3.1) and (2.2),

$$\frac{d\sigma}{dr}^{h=1} - \frac{d\sigma}{dr}^{h=-1} = \frac{16\pi\alpha^2}{Q^2} R(Q^2) \sum_i{}' [b a_i Q_i + R(Q^2) ab (a_i^2 + b_i^2)]$$
$$\times \int_{\sqrt{r}}^{1} \frac{dx}{x} [I_i(r,x) + I_{\bar{i}}(r,x)] \int_{y_0}^{1-y_0} y^2 dy . \tag{3.3}$$

The y-integration limits correspond to coverage of both $q_0 > 0$ and $q_0 < 0$ regions. Notice that terms propertional to h cos θ in (3.1) can be probed by correlating measurements of both helicity and charge symmetry, however difficult that may be.

Numerical results are again left for the next section. We should add that higher-order electromagnetic corrections do not contribute to $\langle h\rangle$ in our model, unlike muon pairs produced in electron-positron colliding beams where both the charge asymmetry and muon polarization get contributions from QED corrections. The difference lies in the fact that we average over quark spins here in contrast to the e^+, e^- beams which are polarized at high energy.

IV. MODEL DEPENDENT ESTIMATES

Our numerical calculations require models for both the parton distribution functions and the Z-boson coupling constants. A reasonable idea of the magnitude of the effects we are interested in ought to be achieved through the parton model of Berman, Bjorken and Kogut[13] and the four-quark version[14] of the Weinberg model for the couplings.

In such a parton model, two independent distributions are assumed, one for the valence quarks and one for the quark-antiquark sea. (The sea is assumed to be SU_3 symmetric.) Specifically:

$$x\,P_p(x) = 2V(x) + \frac{3}{4}S(x),$$

$$x\,P_n(x) = V(x) + \frac{3}{4}S(x), \qquad (4.1)$$

$$P_{\bar{p}}(x) = P_{\bar{n}}(x) = P_{\bar{\lambda}}(x) = P_{\lambda}(x) = \frac{3}{4x}S(x),$$

with

$$V(x) = 1.1\sqrt{x}\,(1-x)^3,$$

$$S(x) = 0.3(1-x)^{7/2}. \qquad (4.2)$$

The coupling model we are using dictates that

$$a = -\frac{1}{\sqrt{2}}(1 - 4\sin^2\theta_W),$$

$$b = -\frac{1}{\sqrt{2}},$$

$$a_p = \frac{1}{\sqrt{2}}(1 - \frac{8}{3}\sin^2\theta_W),$$

$$a_n = a_\lambda = -\frac{1}{\sqrt{2}}(1 - \frac{4}{3}\sin^2\theta_W),$$

$$b_p = -b_n = -b_\lambda = \frac{1}{\sqrt{2}} . \tag{4.3}$$

For the quarks,

$$Q_p = -2Q_n = -2Q_\lambda = \frac{2}{3} . \tag{4.4}$$

Here θ_w is the γ-Z mixing angle, bound empirically[3] according to $\sin^2 \theta_w < 0.4$, and fixes the mass m_Z through

$$m_Z^2 = \frac{1}{\sqrt{2}\, G} \left(\frac{e}{\sin 2\theta_w} \right)^2 . \tag{4.5}$$

However, we shall drop this condition in order to display separately the dependence on $m_Z{}^2$ and the V-A admixture for fixed $\frac{g_Z{}^2}{m_Z{}^2}$.

In Figs. 3 and 4, we plot A^{weak} as a function of $r = Q^2/s$ for $\theta_w = 0^o$ and $\theta_w = 30^o$ (corresponding to $m_Z = \infty$ and 87 GeV/c^2, respectively, in the Weinberg model). The center of mass energy is $s_{ISR} = (54 \text{ GeV})^2$ in Fig. 3 and $s_{Isabelle} = (400 \text{ GeV})^2$ in Fig. 4. No cutoff is made ($y_0 = 0$). Figures 5 and 6 show the analogous distribution for the average helicity.

It is seen that both weak effects are substantial, with interesting m_Z, a/b and s dependence. As expected, there is a striking difference between the c.m. energies, 54 and 400. Except for a boson mass just above threshold ($m_Z \approx 50$ GeV/c^2), the one photon contribution dominates at ISR energies, while the weak amplitude plays the major role at 400 GeV. For $\theta_w = 0^o$, a = b and the pure V-A weak coupling picks out a pure helicity state for the muons; thus the 100% polarization seen in Fig. 6 is expected. The other choice, $\theta_w = 30^o$, corresponds to a = 0 and the V, A interference term vanishes as the purely axial weak transition becomes predominant.

An encouraging aspect of our estimate of A^{EM} is its smallness relative to A^{weak}. We find it to be about -0.4% at $\sqrt{s} = 54$ (for fixed percentage energy resolution, A^{EM} is only weakly dependent on r). Because of the growing importance of the neutral current in the symmetric part of the cross section, A^{EM} is essentially zero at $\sqrt{s} = 400$.

We should mention that raising the cutoff to $y_o = \frac{1}{4}$ reduces A^{weak} by about 40% and A^{EM} by about 65%. The average helicity is unaffected as long as the cutoff is independent of x.

V. CONCLUDING REMARKS

After all is said and done, the qualitative features seen here are easy to understand. The weak amplitude will eventually dominate at high enough energy and, for example, a simple V-A lepton coupling leads to 100% polarization. We should point out that only a restricted range of m_Z values are relevant: if m_Z^2 is not large compared with Q^2, the obvious thing to consider is its direct production.[15] In the Weinberg model there is an experimental upper limit[3] implied by $\sin^2 \theta_W \geq 0.1$. Although $\theta_W = 30^o$ corresponds to m_Z small enough to be produced in the energy regime considered here and although $\theta_W = 0^o$ ($m_Z = \infty$) is inconsistent with the upper limit, the results for an intermediate m_Z value can be extrapolated from our two extreme cases. One should keep in mind that the resonance enhancement of the cross section for $Q^2 \approx m_Z^2$ is hidden in ratios like A and <h>. (Dips, rather than peaks, can appear.)

It seems reasonable to have neglected quark as well as lepton masses in our calculations, in view of the high energies considered.[16] Besides, we have checked that the electromagnetic contribution A^{EM} is changed little even for masses as large as 10% of $\sqrt{Q^2}$. Spurious $\theta = 0$ divergences are washed out in the integrations. Even if our use of the parton model is inadequate for the two-photon estimate, we would still expect electromagnetic contributions to charge asymmetries to have a rather different angular dependence [see, for example, F(y)] than that due to the neutral weak current. Measurements of the transverse momentum distribution of the leptons ought to be useful in separating the two components. Also of importance is the fact that A^{EM} ought to scale (be independent of Q^2) in the absence of weak currents.

The alert reader might wonder about the two-photon exchange diagrams[17] shown in Fig. 7. In our parton model, these do not interfere with the lowest-order amplitude and appear to play no crucial role in our calculations. However, remember that huge contributions from such graphs and other symmetric radiative corrections will change significantly the denominators in our ratios.

A more serious criticism of our estimate is the following. The dominant contribution was found to occur through exchange of one hard photon and one soft photon. There is no reason to believe that the soft photon probes the internal structure of the proton; a more reasonable picture might be one in which a hard photon is created by parton annihilation and a soft photon by hadron bremsstrahlung as illustrated in Fig. 8. However, one might guess that this would lead to the same order of magnitude for the asymmetry effect, although qualitative features could be different. For example, the relation between the asymmetries in energy and momentum [c.f., Eq. (2.7)] is a specific prediction of parton annihilation, it holds for the interference of Figs. 1 and 2 but is not expected to hold for the interference of Fig. 1 with Fig. 7.

Parity violation is, of course, a cleaner signature of the weak interaction. In view of the difficulty of polarization measurements one might look for an asymmetry of the form

$$\langle [\bar{p}_+ x \bar{p}_-] \; \bar{p}_{beam} \, (\bar{Q} \cdot \bar{p}_{beam}) \rangle \quad .$$

However, such an effect is also odd under time reversal. In an inclusive experiment it could be observed only in the presence of strong interactions in the initial pp state. Such effects, of course, cannot be evaluated in the parton model, which neglects them by definition, but to the extent that the parton model is empirically valid, their contribution is likely to be small.

ACKNOWLEDGMENTS

We have benefited from discussions with L. Lederman. Parts of this work were performed at the Aspen Center for Physics and at the CERN Theory Division. R. W. B and M. K. G. , respectively, are happy to thank these institutions for their hospitality.

FIGURE CAPTIONS

Fig. 1 (a) Quark annihilation and (b) quark bremsstrahlung diagrams for $pp \to \ell^+\ell^- X$.

Fig. 2 Some higher-order electromagnetic diagrams contributing to the charge asymmetry in $pp \to \ell^+\ell^- X$.

Fig. 3 Lepton charge asymmetry due to neutral currents in $pp \to \ell^+\ell^- X$, at a c.m. energy of 54 GeV for two values (0^o and 30^o) of θ_w. We have put $y_0 = 0$.

Fig. 4 Lepton charge asymmetry at a c.m. energy of 400 GeV.

Fig. 5 Average lepton helicity due to neutral currents in $pp \to \ell^+\ell^- X$, at a c.m. energy of 54 GeV for two values (0^o and 30^o) of θ_w and $y_0 = 0$.

Fig. 6 Average lepton helicity for a c.m. energy of 400 GeV.

Fig. 7 A two-photon exchange diagram which does not interfere with quark annihilation amplitudes.

Fig. 8 Higher-order electromagnetic diagrams with one hard photon from parton annihilation and one soft photon from external bremsstrahlung.

REFERENCES

[1]For a survey, see the Proceedings of the XVI Conference on High Energy Physics (NAL 1972).

[2]F.J. Hasert, et al., Phys. Lett. 46B, 121 and 138 (1973); A. Benvenuti, et al., preprint.

[3]For some experimental consequences of gauge theories and their present status, see C.H. Llewellyn Smith, TH.1710-CERN and B.W. Lee, NAL-Conf-73/63-THY.

[4]The classic model in which this is true is that of S. Weinberg, Phys. Rev. Letters 19, 1264 (1967) and 27, 1688 (1971).

[5]See, for example, V.K. Cung, A.K. Mann and E.A. Paschos, Phys. Lett. 41B, 355 (1972); J. Godine and A. Hankey, Phys. Rev. D6, 3301 (1972).

[6]In particular, Isabelle at BNL.

[7]S.D. Drell and T.M. Yan, Phys. Rev. Letters 25, 316 (1970), and Ann. Phys. (N.Y.), 66, 578 (1971).

[8]B.J. Blumenfield, et al., (CERN-Columbia-Rockefeller collaboration) "Results on Large Transverse Momentum Phenomena", presented at the Vanderbilt Conference, March 26-28, 1973; J.H. Christenson, et al., Phys. Rev. Letters 25, 316 (1970).

[9]I. B. Khriplovich, Novosibirsk preprint, submitted to the Chicago-Batavia Conference, 1972; R. W. Brown, et al., Phys. Lett. 43B, 403 (1973); D. A. Dicus, Phys. Rev. D8, 890 (1973); F. A. Berends, K. J. F. Gaemers, and R. Gastmans, Leiden preprint (1973).

[10]R. W. Brown and K. O. Mikaelian, CWRU preprint (1973).

[11]J. D. Bjorken and E. A. Paschos, Phys. Rev. 185, 1975 (1969); J. Kiskis, Phys. Rev. D8, 2129 (1973).

[12]The exact calculations of F. A. Berends, et al., (Ref. 9) verify this.

[13]S. Berman, J. D. Bjorken and J. B. Kogut, Phys. Rev. D4, 3388 (1971).

[14]S. Weinberg, Phys. Rev. D5, 1412 (1972). We assume there are no charmed quarks in the proton.

[15]R. L. Jaffe and J. R. Primack, Nucl. Phys. (to be published).

[16]We could not do this in the charge symmetric corrections because of the logarithmic mass divergences. See, e.g., J. Kiskis, Ref. 11.

[17]See the extensive work of M. S. Chen, I. J. Muzinich, and H. Terazawa, and T. P. Cheng, Phys. Rev. D7, 3485 (1973).

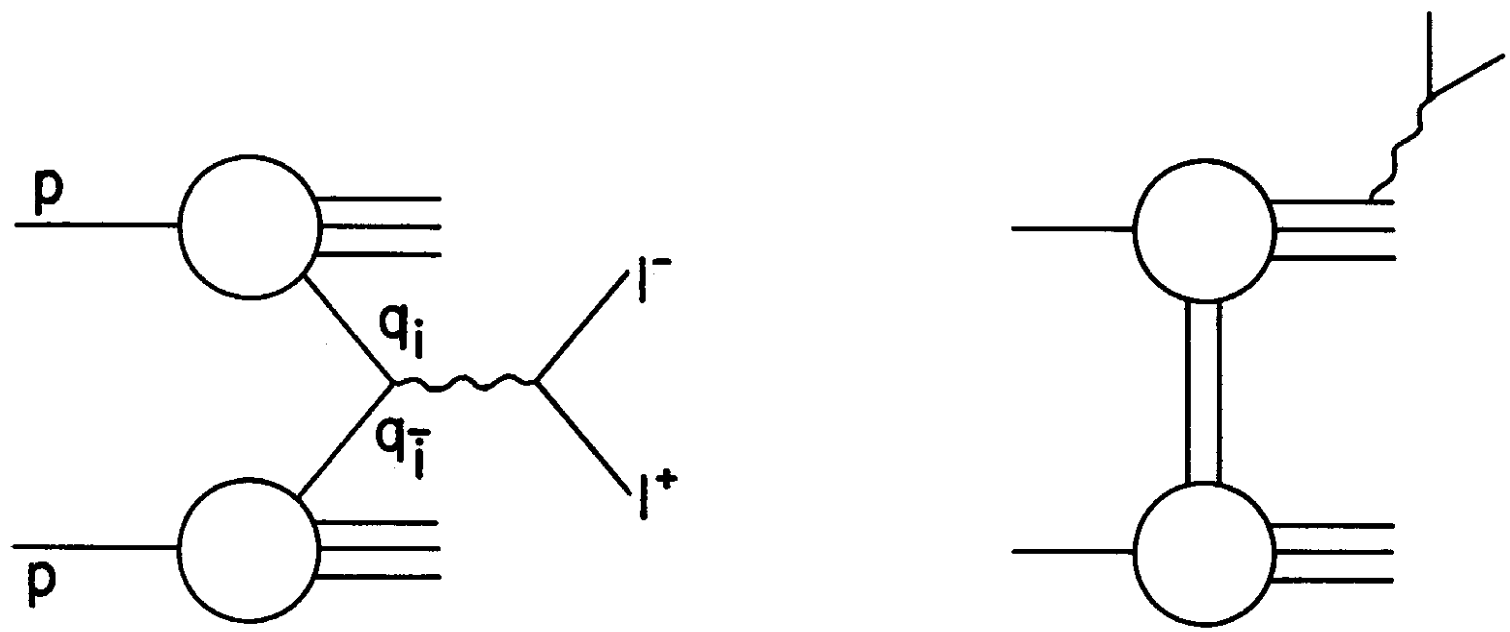

(a) (b)

FIG. 1

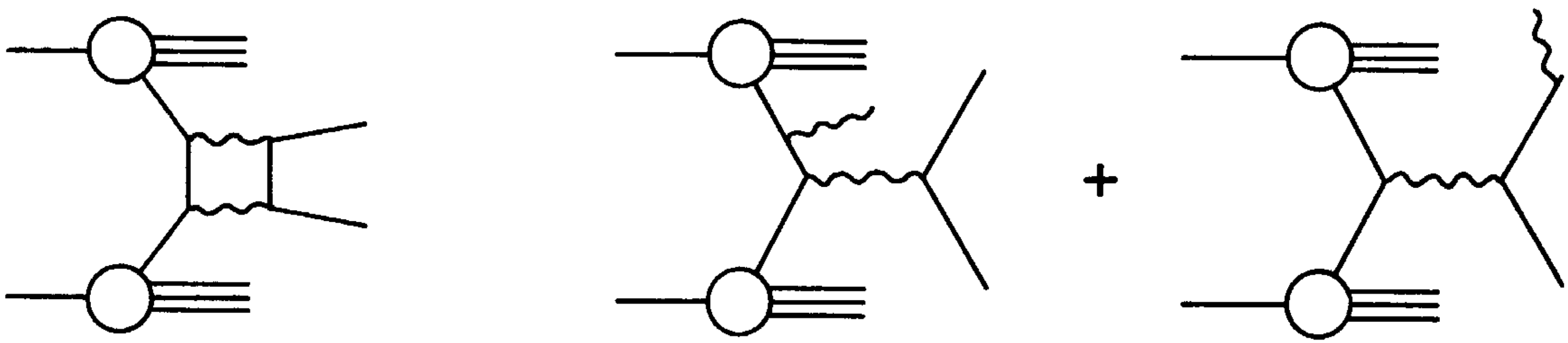

FIG. 2

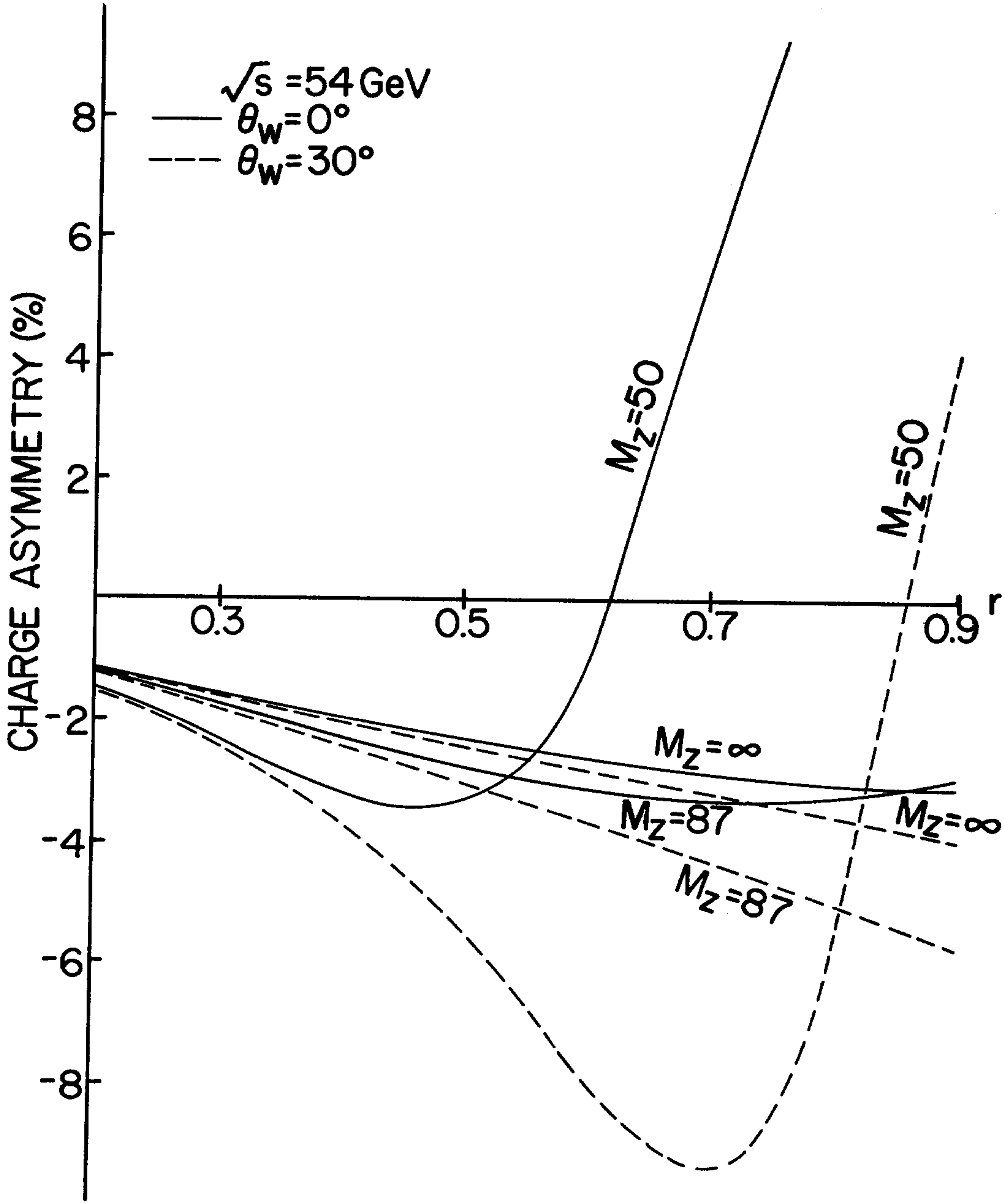

√s =54 GeV
θw=0°
θw=30°
CHARGE ASYMMETRY (%)
8
6
4
2
-2
-4
-6
-8
0.3
0.5
0.7
0.9
r
MZ=50
MZ=50
MZ=∞
MZ=87
MZ=∞
MZ=87

FIG. 3

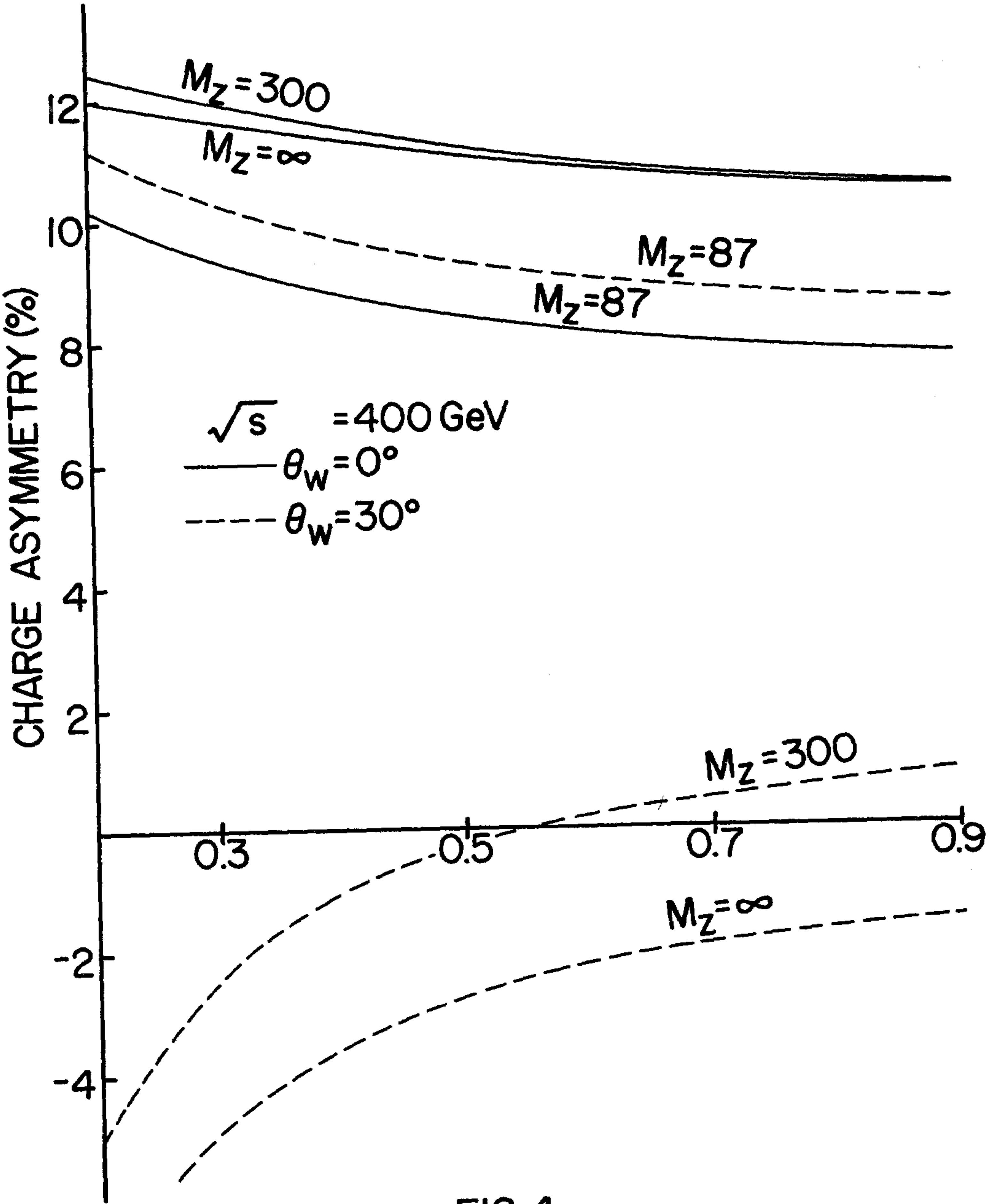
CHARGE ASYMMETRY (%)
12
10
8
6
4
2
-2
-4
$M_Z=300$
$M_Z=\infty$
$M_Z=87$
$M_Z=87$
$\sqrt{s}$ =400 GeV
$\theta_W=0°$
$\theta_W=30°$
$M_Z=300$
$M_Z=\infty$
0.3
0.5
0.7
0.9
r

FIG. 4

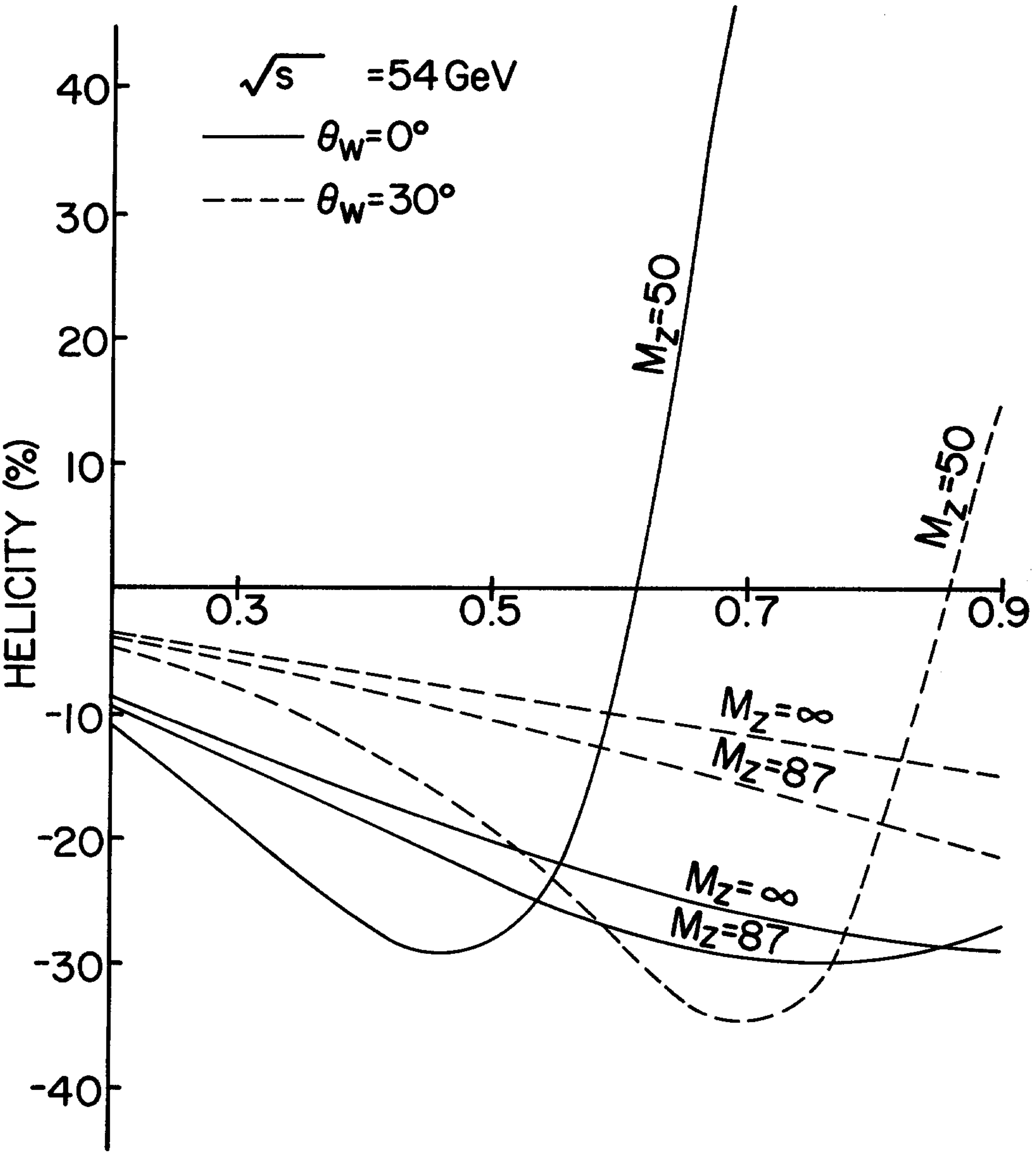
$\sqrt{s}$ =54 GeV
θ_W=0°
θ_W=30°
HELICITY (%)
40
30
20
10
-10
-20
-30
-40
0.3
0.5
0.7
0.9
M_Z=50
M_Z=50
M_Z=∞
M_Z=87
M_Z=∞
M_Z=87

FIG. 5

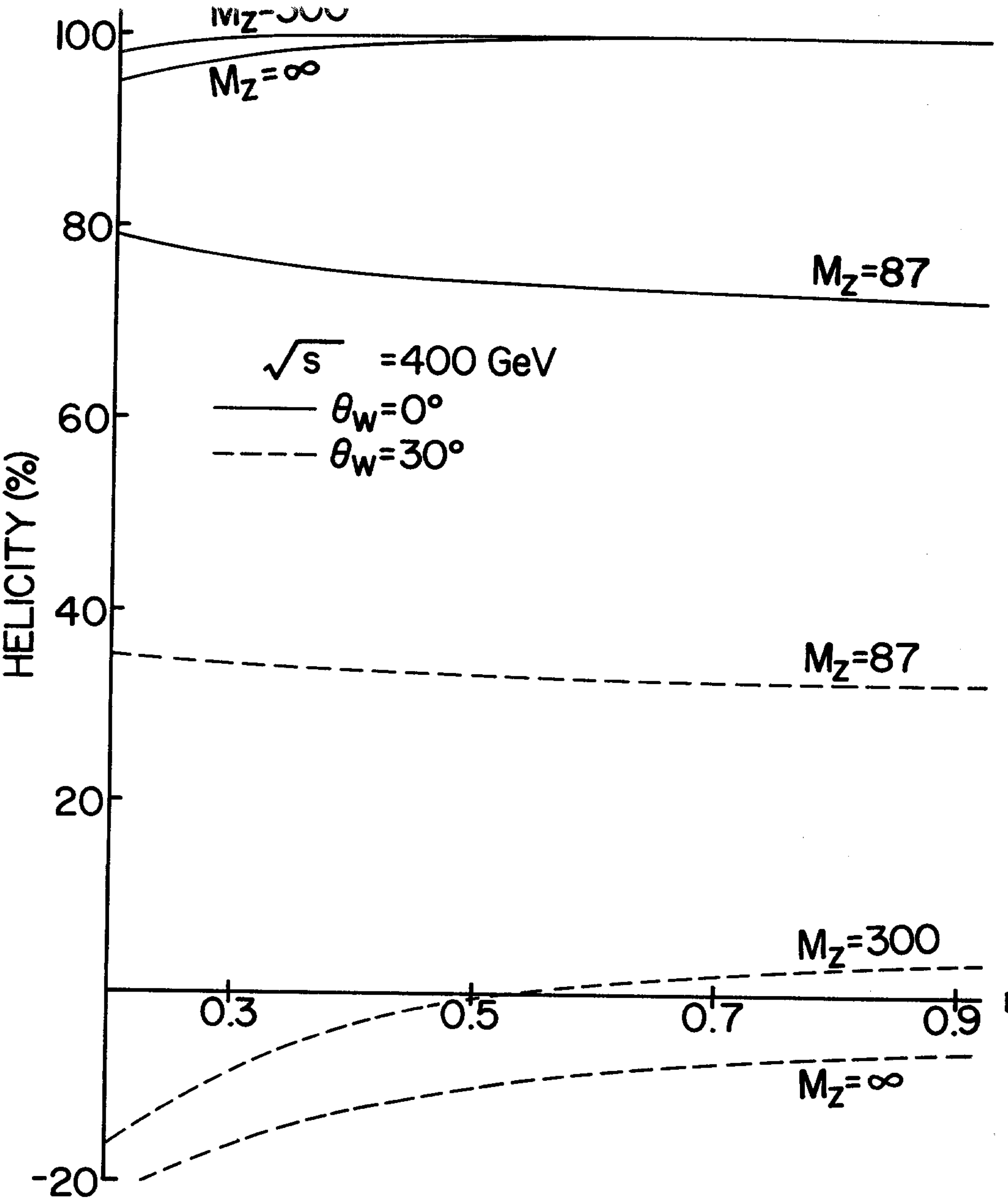

$M_Z=300$
100
$M_Z=\infty$
80
$M_Z=87$
$\sqrt{s}$ =400 GeV
$\theta_W=0°$
$\theta_W=30°$
60
HELICITY (%)
40
$M_Z=87$
20
$M_Z=300$
0.3
0.5
0.7
0.9
r
$M_Z=\infty$
-20

FIG. 6

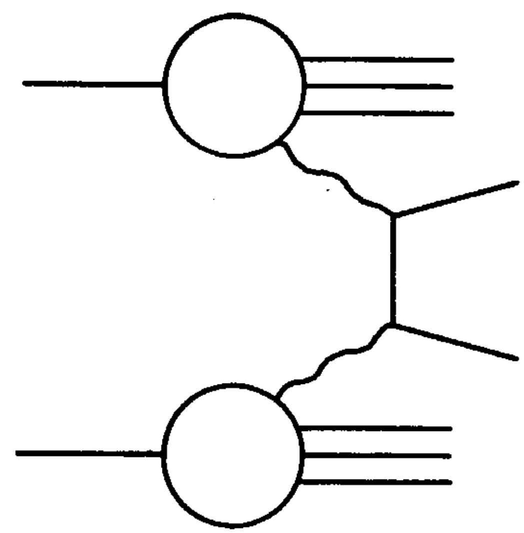

FIG. 7

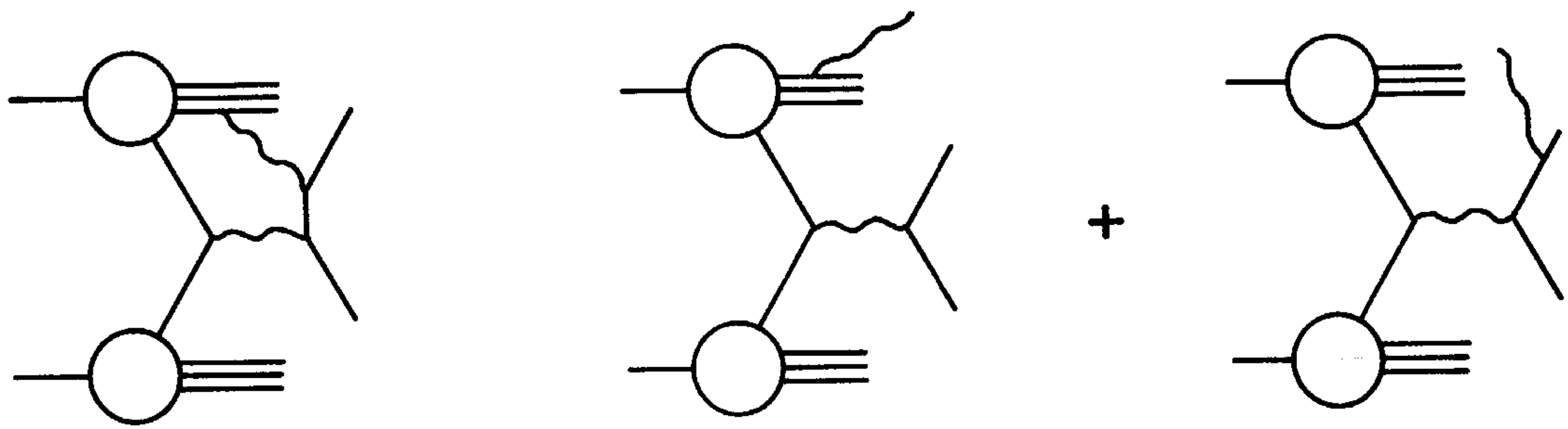

FIG. 8